

Towards User-Independent DTI Quantification

Jan Klein^a, Hannes Stuke^a, Jan Rexilius^a, Bram Stieltjes^b,
Horst K. Hahn^a, and Heinz-Otto Peitgen^a

^aMeVis Research, Center for Medical Image Computing, Bremen, Germany

^bGerman Cancer Research Center, Department of Radiology, Heidelberg, Germany

ABSTRACT

Quantification of diffusion tensor imaging (DTI) parameters has become an important role in the neuroimaging, neurosurgical, and neurological community as a method to identify major white matter tracts afflicted by pathology or tracts at risk for a given surgical approach. We introduce a novel framework for a reliable and robust quantification of DTI parameters, which overcomes problems of existing techniques introduced by necessary user inputs. In a first step, a hybrid clustering method is proposed that allows for extracting specific fiber bundles in a robust way. Compared to previous methods, our approach considers only local proximities of fibers and is insensitive to their global geometry. This is very useful in cases where a fiber tracking of the whole brain is not available. Our technique determines the overall number of clusters iteratively using an eigenvalue thresholding technique to detect disjoint clusters of independent fiber bundles. Afterwards, possible finer substructures based on an eigenvalue regression are determined within each bundle. In a second step, a quantification of DTI parameters of the extracted bundle is performed. We propose a method that automatically determines a 3D image where the voxel values encode the minimum distance to a reconstructed fiber. This image allows for calculating a 3D mask where each voxel within the mask corresponds to a voxel that lies in an isosurface around the fibers. The mask is used for an automatic classification between tissue classes (fiber, background, and partial volume) so that the quantification can be performed on one or more of such classes. This can be done per slice or a single DTI parameter can be determined for the whole volume which is covered by the isosurface. Our experimental tests confirm that major white matter fiber tracts may be robustly determined and can be quantified automatically. A great advantage of our framework is its easy integration into existing quantification applications so that uncertainties can be reduced, and higher intrarater- as well as interrater reliabilities can be achieved.

Keywords: Diffusion Tensor Imaging, Quantification, Fiber Clustering, Fiber Tracking

1. INTRODUCTION

The possibility of quantifying diffusion tensor imaging (DTI) parameters has established a whole range of new clinically useful applications and research studies. For example, color-coded maps of parameters like fractional anisotropy (FA) computed from DTI data were successfully employed in several studies, where it has been shown that modified values of FA, relative anisotropy, or diffusion strength are an indicator of diseases affecting white matter tissue.¹⁻³

1.1 DTI Quantification

A pointwise assessment of DTI parameters was proposed along a single streamline combined with a visualization of uncertainties by Jones et al.⁴ Other quantification algorithms¹⁻³ use a manual definition of one or more ROIs, which cover a certain fiber bundle at some slices of the image data. Within such ROIs, an average parameter can be computed from several single values. Schlueter et al. extended standard ROI-based techniques by considering partial volume effects so that fibrous and non-fibrous tissue can be classified.⁵ Recently, Niethammer et al. have shown how to define fiber bundles implicitly and how to compute their parameters as integrals.⁶

However, it is often desirable to determine the parameters along a whole fiber bundle so that several ROIs have to be drawn manually via a multi-planar reconstruction. Because this process is very time-consuming and

Further author information: (Send correspondence to Jan Klein)
Jan Klein: E-mail: jan.klein@mevis.de, Telephone: 49 421 218 8902

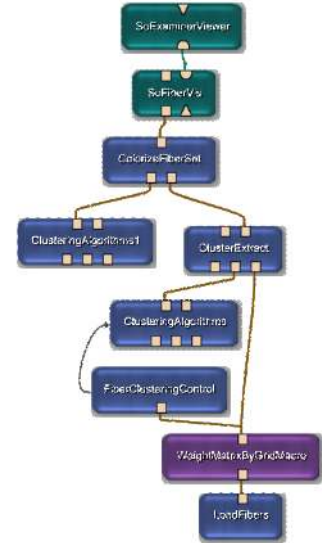
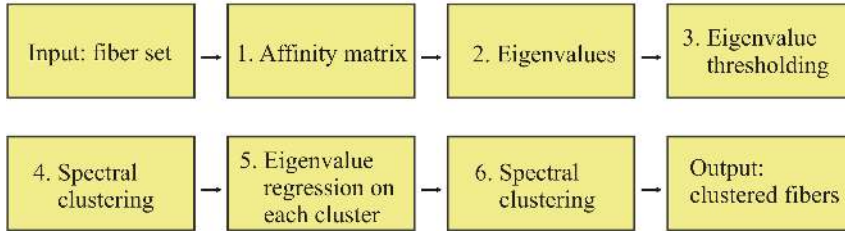


Figure 1. Left: algorithmic idea of our novel hybrid fiber clustering method. From an affinity matrix that has been computed by a fiber grid (step 1), eigenvalues are computed using a singular value decomposition (step 2). Afterwards, the number of coarse cluster is determined by Eigenvalue thresholding (step 3) and spectral fiber clustering is performed (step 4). Then, the number of finer structures within each cluster is computed by Eigenvalue regression (step 5). Finally, spectral clustering is done on each coarse cluster (step 6). Right: corresponding MeVisLab network. The associated algorithms are encapsulated as modules. The connections represent the data flow.

error-prone, a semi-automatic algorithm, where ROIs are placed on axial, sagittal, or coronal slices between two predefined ROIs automatically, has been proposed by Aoki et al.⁷ Other techniques are not limited to the alignment of ROIs or VOIs used for the local assessment and computation of parameters. Fillard et al.⁸ compute an average DTI parameter from several single values that all have the same geodesic distance from a user-defined origin. An automatic quantification of DTI-parameters along fiber bundles has been proposed by Klein et al.,⁹ where the parameters are computed depending on the local curvature. However, partial volume effects are considered only to a limited extend.

Especially for comparisons between individuals it is necessary to determine the parameters in a very robust and reliable way. Therefore, O'Donnell et al. propose a method for automatic generation of white matter tract arc length parameterizations, based on learning a fiber bundle model from tractography from multiple subjects.¹⁰ They make use of a fiber clustering algorithm to group anatomically similar or related fibers into bundles.

1.2 Fiber Clustering

Fiber clustering algorithms^{11–21} allow for extracting specific bundles of interest that can be used for quantification. Although this seems to be the ideal basis for reducing undesirable bias introduced by the user in the quantification process, there are still some problems. Most clustering techniques like hierarchical clustering, partitioning clustering, elongated clustering, or self-organizing maps require a predefined number of clusters, which has to be set by the user. Because this can be a difficult task, an implausible number could be utilized, which does not correspond to an anatomically meaningful separation of the fiber bundles. Thus, fibers corresponding to a certain fiber bundle could be separated into two or more different clusters. Figure 5 i illustrates the problem.

As a consequence, spectral clustering algorithms have been developed, which allow to determine the number of clusters automatically.^{13,16,20} Unfortunately, the results may be user-dependent, if the clustering is not performed on all available fibers. That means, e.g., a large bundle, which has been divided into a fixed number of clusters, may be differently clustered if adding an anatomically different bundle to the set (Figure 5 ii). Obviously, this behavior, which mainly results from the automatic detection of the number of clusters, is not desired.

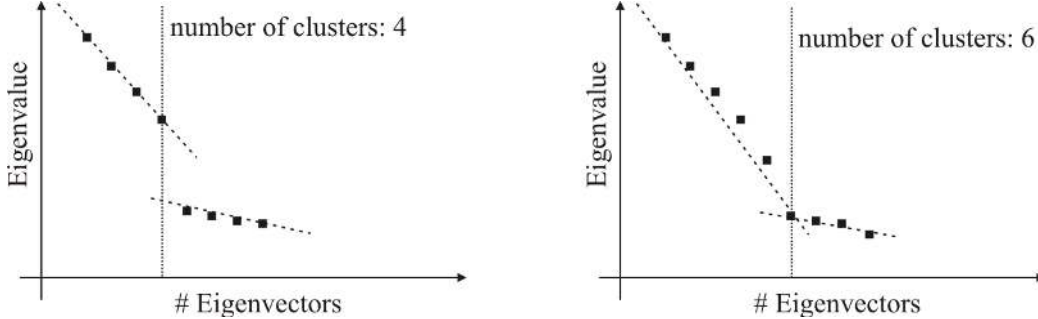


Figure 2. The eigenvalue regression is powerful tool for detecting the number of finer substructures within fiber sets. However, it may not always be a robust tool for computing the number of clusters automatically. In the illustrated example, only a single fiber is appended to a given fiber set, but the number of clusters increases by two. This is due to the fact that the method is based on geometrical affinities, but not on meaningful anatomical relations.

A framework for a reproducible fiber bundle selection, has been proposed by Blaas et al.²² However, manual user interaction is still necessary. Algorithms using the underlying tensor field for clustering²³ may have a high running time, which is not desirable in clinical applications.

1.3 Contributions

We introduce a novel hybrid clustering technique that determines the number of clusters iteratively. In a first step, only coarse clusters are computed from which afterwards finer structures are extracted. An algorithmic overview is given in Figure 1. After extracting a specific fiber bundle, we determine the parameters of interest by a quantification method that has been introduced by Schlueter et al.⁵ We had to extend this method as it was only designed to determine DTI parameters within a single user-defined ROI and not along a predefined fiber bundle. The rest of this paper is organized as follows: in Section 2 we introduce how to extract a specific fiber bundle and how to automatically quantify DTI parameters by considering partial volume effects. Section 3 summarizes the results and gives a comparison of our new hybrid clustering technique with spectral algorithms. The last section concludes our work and gives some ideas for future work.

2. METHODS

2.1 Fiber Bundle Extraction

Using a deflection-based fiber tracking algorithm,²⁴ fiber bundles can be reconstructed from DTI data. Afterwards, an affinity matrix representing the similarity of each pair of fibers is computed by a fiber grid.²⁰ As it has been shown, the eigenvalue regression technique may be useful for computing finer substructures within larger fiber bundles.²⁰ However, this technique is sensitive to disjoint clusters, so that it may not always be used for computing an anatomically meaningful number of clusters. This sensitivity is due to the fact that the number of eigenvalues of the affinity matrix and, thus, of the number of clusters can change (Figure 2).

To overcome this problem and to decrease the influence of independent fiber bundles that do not influence the local clustering if they do not introduce new local geometrical information, disjoint clusters are determined in a first step (Figure 1). From graph theory it is well-known that clusters in graphs correspond to large eigenvalues of the affinity matrix. There, clusters with eigenvalues close to one are very different among each other. As a consequence, the isolation of such clusters can easily be achieved by a simple thresholding of the eigenvalues where the number k_1 of clusters is computed by the number of eigenvalues, which are larger than a certain threshold t :

$$k_1 := \{\#e_i | e_i > t \forall i \in \{1, \dots, n\}\} \quad (1)$$

where e_i denotes the i -largest eigenvalue and n the number of all fibers. As an alternative, an eigengap detector has been implemented where the largest gap between two consecutive eigenvalues defines the number of clusters:

$$k_1 := \arg_{i \in \{1, \dots, n-1\}} \{e_i - e_{i+1}\}. \quad (2)$$

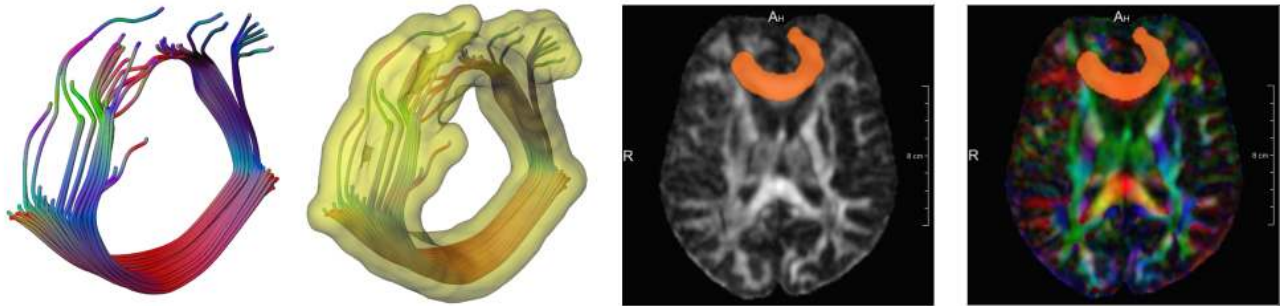


Figure 3. An isosurface with a predefined distance to the selected fibers is used to determine a 3D mask image. This image is used instead of manually defined ROIs for the classification algorithm. In the two figures on the right, the mask is shown as an overlay on a FA map as well as on a color-coded DTI map corresponding to the fiber bundle shown on the left.

Using this number, spectral fiber clustering^{13,16,20} can be applied to the fiber set. Finally, for each cluster, its own number of finer structures is defined by an Eigenvalue regression, i.e., all eigenvalues e'_i of each cluster are computed and are split into two subsets so that for each set the regression lines have minimal distance to the eigenvalues e'_i . For that purpose, a submatrix is computed from the original affinity matrix so that the time for computing the eigenvalues e'_i is reduced.

2.2 DTI Quantification

Single bundles, which are extracted by the technique described above, may be quantified by averaging the parameters of interest along the mean curvature of the bundle.⁹ However, partial volume effects are not modeled by this approach, and areas where no fibers have been tract are not taken into account. Therefore, we developed a method based on an algorithm that was previously used for the quantitative analysis of DTI parameters within single user-defined ROIs.⁵ Within such an ROI, a probabilistic mixture model is assumed including the pure tissue classes, fiber and background, as well as a mixture class modeling partial volume artifacts.

To perform an automatic quantification using this method, we propose several extensions. In a first step, the reconstructed fibers are voxelized into an isotropic grid, on which a Euclidean distance transformation is applied. This yields a 3D image where each voxels value encodes the minimum distance to a reconstructed fiber. Afterwards, an isosurface is determined from this image with a predefined distance to the fibers. Finally, the isosurface is voxelized and voxels within the surface are filled. This 3D mask image can then be used instead of the user-defined ROIs as illustrated in Figure 3. Note that the classification algorithm⁵ requires a mask, where fiber, partial volume, as well as background are included in order to compute a correct result. This explains the fact that we compute an isosurface with a certain margin around the fibers. The result is very stable for a broad spectrum of values for the margin, see Figure 4. However, if the size of the margin is chosen much too large, the classification algorithm will fail as shown in Figure 7.

The classification and quantification of the tissue classes (fiber, background and mixture) can be performed per slice using the precomputed 3D mask. In this case, the user only has to slice through the image data and may view the resulting quantification parameters (Figure 4). As an alternative, a single DTI parameter may be determined for the whole volume which is covered by the isosurface.

3. RESULTS

We have implemented all algorithms in C++ on top of MeVisLab.²⁵ An excerpt of the corresponding MeVisLab network encapsulating the automatic extraction of fiber bundles is shown in Figure 1 (right).

In our experiments we would like to test, if geometrically and anatomically independent fiber bundles are reproducible clustered if the initial fiber set for clustering is changed, i.e., if other bundles are added or deleted from the fiber set. Using a deflection-based fiber tracking algorithm,²⁴ major white matter fiber tracts of a

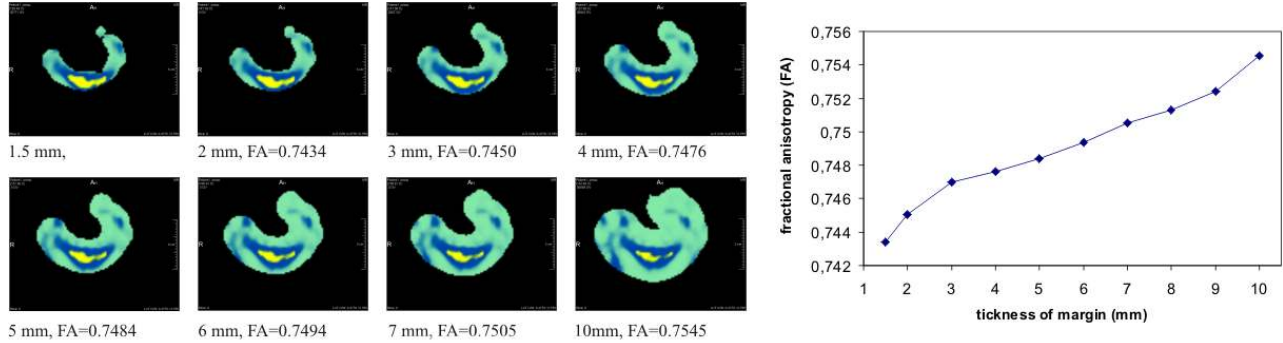


Figure 4. Left: an isosurface with a predefined distance to the fibers can be used to define a 3D mask used for the classification process. Three different tissue classes (fiber=yellow, background=cyan, partial volume=blue) are computed using a probabilistic mixture model. The fractional anisotropy (FA) values shown in this example are measured only for pure fiber tissue. Right: the plot shows that if increasing the margin around the fibers, the resulting quantification only slightly changes. The increase seems to be linear and is only 1.5 percent if increasing the margin from 1.5mm to 10mm.

human brain are determined using single seed regions. This procedure results in separate fiber bundles and it allows for defining several configurations with different bundles. That means, we are able to select some specific fiber sets and treat them all as a single fiber set used for our clustering algorithm. As a consequence, we can create several such fiber sets that consist of different constellations with respect to the original whole brain fiber tracking.

In the following step, our hybrid clustering technique can be applied to each set. Our measurements show that independent of the current selection, the originally indented fiber bundles are determined correctly (Figure 6). In contrast, if skipping step 4 and step 5 (Figure 1), different clustering results are achieved depending on the current selection of the fiber bundles (Figure 5). In most cases, our experimental results show that the simple eigenvalue thresholding technique ($t := 0.92$) is superior to the eigengap detector, where different subclusters are determined depending on the initial selection.

In a second experiment, a certain fiber bundle with adjacent fibers is determined by defining seed ROIs that exceed the actual fiber bundle. Our results confirm that the bundle of interest can only be correctly extracted from the other fibers with our hybrid clustering.

Finally, we perform an automatic quantification of DTI parameters such as the FA value along the extracted bundle. This process is repeated for different initial fiber sets and different seed regions, respectively. A high intrarater-reliability $r > 0.96$ can be achieved.

4. CONCLUSIONS AND FUTURE WORK

Previous quantification algorithms depend on user-defined ROIs, need extensive manual adjustments or are only able to quantify parameters without considering the corresponding fiber bundles which can be obtained by fiber tracking. More sophisticated techniques are sensitive to the selection of user-defined ROIs needed for seeding the fiber tracts or for computing average parameters.

Our novel approach may be used for reproducible and robust quantification of DTI parameters along fiber bundles. We have proposed a fiber clustering method that constitutes the basis for user-independent quantification tasks. The quantification is based on a classification algorithm that takes into account partial volume effects. As a consequence, the quantification process can be enhanced and uncertainties can be reduced.

We are aware of the fact that, similar to approaches where the underlying tensor field is used for the actual clustering step, we cannot guarantee a user-independent quantification process under all circumstances, as for the clustering process only geometric affinity measures are used without knowledge about the underlying anatomy.

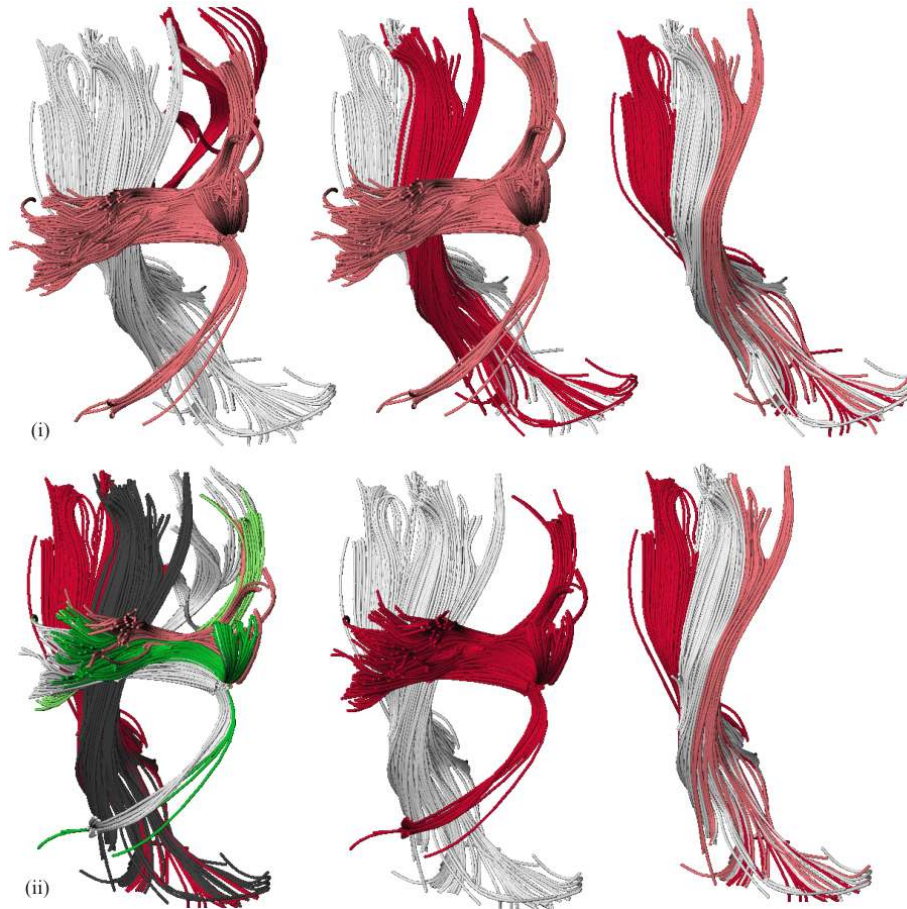


Figure 5. The figure illustrates problems with defining the number of clusters. In this example, we used a standard spectral clustering algorithm. (i) The number of clusters is set to three for different fiber sets. Only for the first fiber set, the clustering leads to anatomically meaningful bundles (pyramidal tract, SLF, and part of the corpus callosum). (ii) Clusters are automatically detected by spectral clustering based on eigenvalue regression. Note that if removing some fibers of the original fiber set, bundles are differently clustered. This is obviously not desired. Fibers are grouped into anatomically meaningful bundles only for the second fiber set, where the pyramidal tract and the superior longitudinal fasciculus (SLF) are separated into single bundles.

For the future, the integration of anatomical information would be a very interesting approach. Nevertheless, several experiments have shown that our new approach is already a powerful tool for grouping white matter connections tracked in DTI images into anatomically meaningful bundles and, thus, allows for a robust quantification process.

REFERENCES

1. A. Tievsky, T. Ptak, and J. Farkas, "Investigation of apparent diffusion coefficient and diffusion tensor anisotropy in acute and chronic multiple sclerosis lesions," *Am. J. Neuroradiol.* **20**, pp. 1491–1499, 1999.
2. R. Stahl, O. Dietrich, S. Teipel, H. Hampel, M. Reiser, and S. Schoenberg, "Assessment of axonal degeneration on alzheimer's disease with diffusion tensor mri," *Radiologe* **43**(7), pp. 566–575, 2003.
3. A. Tropine, G. Vucurevic, P. Delani, S. Boor, N. Hopf, J. Bohl, and P. Stoeter, "Contribution of diffusion tensor imaging to delineation of gliomas and glioblastomas," *J Magn Reson Imaging* **20**(6), pp. 905–912, 2004.
4. D. Jones, A. Travis, G. Eden, C. Pierpaoli, and P. Bassar, "PASTA: Pointwise assessment of streamline tractography attributes," *Magn. Reson. Med.* **53**, pp. 1462–1467, 2005.

5. M. Schlueter, B. Stieltjes, H. K. Hahn, J. Rexilius, O. Konrad-Verse, and H.-O. Peitgen, "Detection of tumour infiltration in axonal fibre bundles using diffusion tensor imaging," *Int J Medical Robotics and Computer Assisted Surgery* **1**, pp. 80–86, 2005.
6. M. Niethammer, S. Bouix, C.-F. Westin, and M. E. Shenton, "Fiber bundle estimation and parametrization," in *MICCAI'06*, pp. 252–259, 2006.
7. S. Aoki, N. K. Iwata, Y. Masutani, M. Yoshida, O. Abe, Y. Ugawa, T. Masumoto, H. Mori, N. Hayashi, H. Kabasawa, S. Kwak, S. Takahashi, S. Tsuji, and K. Ohtomo, "Quantitative evaluation of the pyramidal tract segmented by diffusion tensor tractography: Feasibility study in patients with amyotrophic lateral sclerosis," *Radiation Medicine* **23**(3), pp. 195–199, 2005.
8. P. Fillard, J. Gilmore, J. Piven, W. Lin, and G. Gerig, "Quantitative analysis of white matter fiber properties along geodesic paths," in *MICCAI'03*, pp. 16–23, 2003.
9. J. Klein, S. Hermann, O. Konrad, H. K. Hahn, and H.-O. Peitgen, "Automatic quantification of dti parameters along fiber bundles," in *Proceedings of Image Processing for Medicine*, pp. 272–276, 2007.
10. L. J. O'Donnell, C.-F. Westin, and A. J. Golby, "Tract-based morphometry," in *Tenth International Conference on Medical Image Computing and Computer-Assisted Intervention (MICCAI '07), Lecture Notes in Computer Science* **4792**, pp. 161–168, (Brisbane, Australia), 2007.
11. J. Shimony, A. Snyder, N. Lori, and T. Conturo, "Automated fuzzy clustering of neuronal pathways in diffusion tensor tracking," in *Soc. Mag. Reson. Med*, 2002.
12. Z. Ding, J. C. Gore, and A. W. Anderson, "Classification and quantification of neuronal fiber pathways using diffusion tensor MRI," *Magn. Reson. Med.* **49**, pp. 716–721, 2003.
13. L. O'Donnell, K. M. M. E. Shenton, M. Dreusicke, W. E. L. Grimson, and C.-F. Westin, "A method for clustering white matter fiber tracts," *AJNR* **27**(5), pp. 1032–1036, 2006.
14. L. J. O'Donnell and C.-F. Westin, "Automatic tractography segmentation using a high-dimensional white matter atlas," *IEEE Transactions on Medical Imaging* **26**, pp. 1562–1575, November 2007.
15. F. Enders, N. Sauber, D. Merhof, P. Hastreiter, C. Nimsy, and M. Stamminger, "Visualization of white matter tracts with wrapped streamlines," in *IEEE Visualization*, pp. 51–58, 2005.
16. A. Brun, H. Knutsson, H. J. Park, M. E. Shenton, and C.-F. Westin, "Clustering fiber tracts using normalized cuts," in *MICCAI'04*, pp. 368–375, 2004.
17. L. Jonasson, P. Hagmann, J.-P. Thiran, and V. J. Wedeen, "Fiber tracts of high angular resolution diffusion mri are easily segmented with spectral clustering," in *Proceeding of ISMRM*, p. 1310, 2005.
18. V. E. Kouby, Y. Cointepas, C. Poupon, D. Rivière, N. Golestani, J.-B. Poline, D. L. Bihan, and J.-F. Mangin, "MR diffusion-based inference of a fiber bundle model from a population of subjects," in *MICCAI'05*, pp. 196–204, 2005.
19. M. Maddah, A. Mewes, S. Haker, W. E. L. Grimson, and S. Warfield, "Automated atlas-based clustering of white matter fiber tracts from DTMRI," in *MICCAI'05*, pp. 188–195, 2005.
20. J. Klein, P. Bittihn, P. Ledochowitsch, H. K. Hahn, O. Konrad, J. Rexilius, and H.-O. Peitgen, "Grid-based spectral fiber clustering," *Proceedings of SPIE Medical Imaging* **6509**, 2007. doi: 10.1117/12.706242.
21. J. Klein, H. Stuke, B. Stieltjes, O. Konrad, H. K. Hahn, and H.-O. Peitgen, "Efficient fiber clustering using parameterized polynomials," *Proceedings of SPIE Medical Imaging to appear*, 2008.
22. J. Blaas, C. P. Botha, B. Peters, F. Vos, and F. H. Post, "Fast and reproducible fiber bundle selection in dti visualization," in *IEEE Visualization*, pp. 59–64, 2005.
23. U. Ziyan, D. Tuch, and C.-F. Westin, "Segmentation of thalamic nuclei from DTI using spectral clustering," in *Ninth International Conference on Medical Image Computing and Computer-Assisted Intervention (MICCAI'06), Lecture Notes in Computer Science 4191*, pp. 807–814, (Copenhagen, Denmark), October 2006.
24. M. Schlueter, O. Konrad, H. K. Hahn, B. Stieltjes, J. Rexilius, and H.-O. Peitgen, "White matter lesion phantom for diffusion tensor data and its application to the assessment of fiber tracking," *Medical Imaging: Image Processing* **5746**, pp. 835–844, 2005.
25. MeVisLab 1.5, "Homepage at: <http://www.mevislab.de>. Accessed January, 2008."

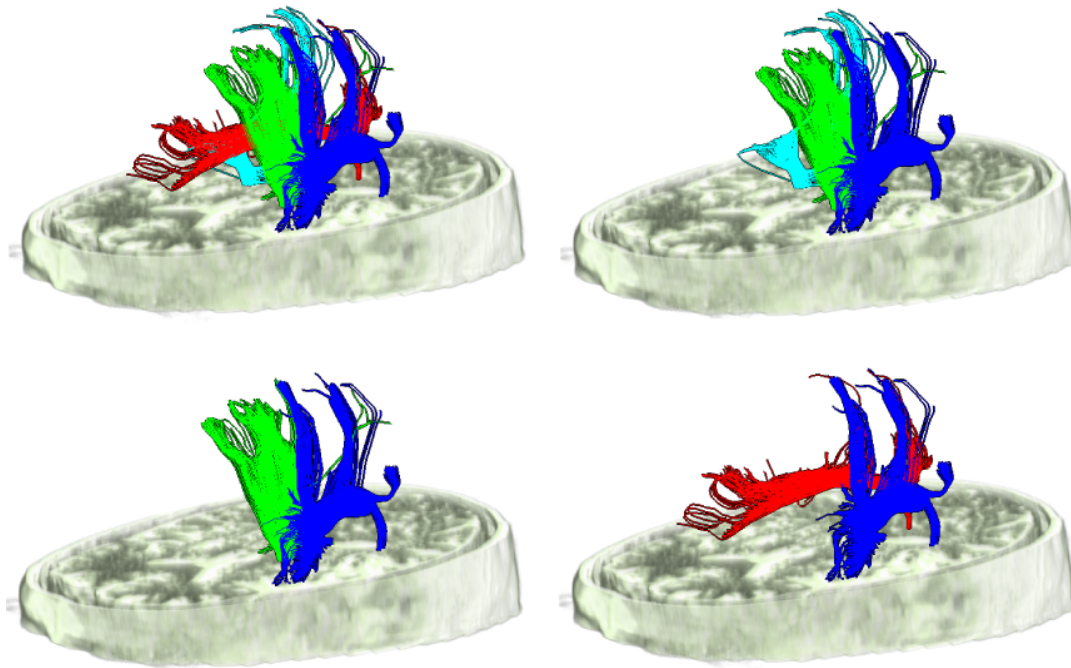


Figure 6. Hybrid fiber clustering (new method). Independent of the original fiber set, our hybrid clustering leads to anatomically meaningful bundles. Thus, specific bundles may be reliable extracted and quantified.

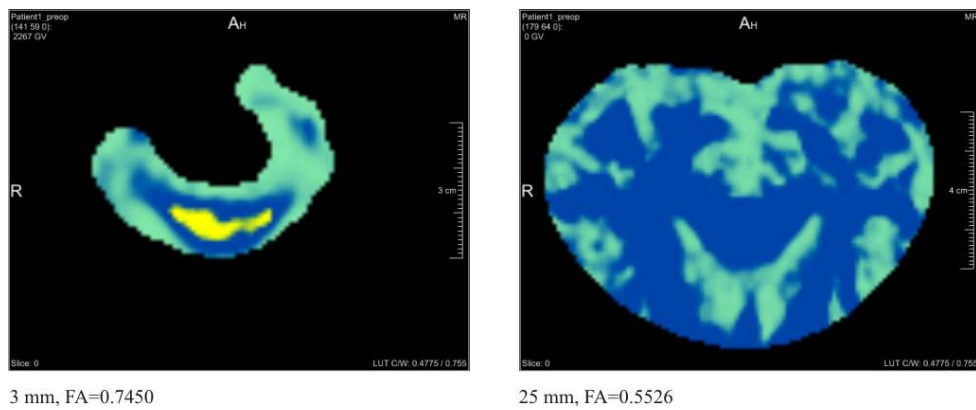


Figure 7. Left: plausible result based on a small margin around the bundle. Right: Large margin leads to incorrect results. In this case, the classification algorithm is not able to distinguish between pure fiber tissue, background, and partial volume.